Paper Number SSC03-X-2

Ongoing Miniaturization Efforts for Ion and Neutral Vector Velocity Instruments

Gregory D. Earle
William B. Hanson Center for Space Sciences, The University of Texas at Dallas,
Box 830688, Richardson, TX 75083, 972-883-6828, earle@utdallas.edu

Jin Liu
Electrical and Computer Engineering Department, The University of Texas at Dallas,
Box 830688, Richardson, TX 75083, jinliu@utdallas.edu

Hao Liu
Electrical and Computer Engineering Department, The University of Texas at Dallas,
Box 830688, Richardson, TX 75083, liuhao@utdallas.edu

Guangbin Zhang
Electrical and Computer Engineering Department, The University of Texas at Dallas,
Box 830688, Richardson, TX 75083, gbzhang@utdallas.edu

Abstract. Future endeavors to study near-Earth space science will involve small satellite fleets deployed in orbits designed to help resolve space-time ambiguities. Key measurements to be made will include three-dimensional drifts of the ionized and neutral constituents of the atmosphere above altitudes of about 150 km. In anticipation of these future missions we have begun to redesign our existing instrumentation for such opportunities. We describe these efforts as related to an ion drift meter instrument that has a long and distinguished flight heritage. Examples of the improvements in power budget and physical size are estimated for the redesigned instrument, and various technological approaches that are conducive to measuring very small currents are discussed. The results are briefly extrapolated to other instrument designs, and comparative estimates based on performance and power requirements are provided.

Introduction

For nearly forty years NASA and other government agencies have flown exploratory space missions that have primarily utilized single, large-scale satellite platforms. In the low Earth orbit (LEO) regime these missions have resulted in many new discoveries, as well as improved understanding of a wide variety of space science phenomena. Representative examples include such diverse topics as large-scale plasma structuring in equatorial spread-F, sprites occurring over large thunderstorms, and the electrodynamics of auroral arcs[1-3].

As a field of study, near-Earth space science has arguably matured to the point that future missions must adopt new approaches in order to enable more detailed study of these phenomena. NASA has recognized this, and has undertaken studies to investigate new mission approaches aimed at moving into a new realm of empirical space science studies.

One example of this new strategy is the Geospace Electrodynamic Connections (GEC) mission, which is designed to determine the temporal and spatial scales at which magnetospheric coupling of energy into low altitude regions occurs, and to assess the thermospheric response to such inputs[4]. This

mission involves 3-4 separate spacecraft to be deployed in elliptical orbits at a high inclination. Comparative measurements between these spacecraft would resolve spatial and temporal effects, which cannot be done using single satellite probes. In order to accomplish this objective it will be necessary to reduce the power budget and mass of the instrumentation flown on each satellite.

In this paper we briefly discuss the specific science goals to be achieved by GEC and similar missions, and we describe some specific instrumentation that will be required to achieve these goals. We then examine general instrumentation issues on small satellites, with particular emphasis on power and mass limitations. Next we focus on a particular instrument, the ion drift meter (IDM), which has a long and successful flight heritage. We compare its present design parameters with those that can be realized through our ongoing miniaturization efforts. We describe these efforts in detail, and provide engineering estimates of the savings in power and mass that we expect to achieve. Finally, we extrapolate these results to several other instrument concepts that will be vitally important to addressing the important science questions.

Science Goals and Instruments

Rather than try to comprehensively address the wide variety of mission scenarios and their attendant orbital constraints, we choose to highlight the GEC mission, which is currently in the planning process for a possible launch in 2008. By highlighting the measurement requirements for this particular mission, we hope to provide specific examples that can logically be carried over to other experiments, even though these may have somewhat different orbits and science objectives.

The science goals for the GEC mission are largely focussed on resolving spatial and temporal ambiguities that arise from single platform space missions. Imagine that a particular signature, such as an abrupt depletion in the plasma density, is observed by a single satellite flying in LEO. Typical LEO orbits have periods of about 90 minutes, and high inclination orbits typically have some small anglular precession in the Earth-fixed frame of reference. Coupled together, these two factors imply that the satellite will not return to the particular region of space in which the irregularity was observed for many hours, or perhaps days depending on the specific orbit. In trying to interpret the data, it is impossible to discern whether the observed feature is a transient event that was coincidentally observed at a particular point in space, or is a long-lived spatial structure that is either stationary or propagating in a particular direction. Most space science missions have been plagued by this problem, which is commonly referred to as a spatial-temporal ambiguity. Through climatological analysis of large amounts of data it is possible to resolve this problem to some degree, but there are some scientific objectives that defy even this approach.

A significant step toward resolving this problem accrues from flying a group of identical satellites along the same orbit track, separated in time. Conversely, some problems may be better studied by flying a group of satellites in a known spatial configuration. Figure 1 illustrates two such scenarios[4]. The illustration on the left shows a configuration called “pearls on a string”, in which the satellites follow the same orbital path, separated in time. The illustration on the right shows the “petal configuration”, in which the same latitude region can be sampled at different altitudes. It is possible to modify the orbits of the satellites between these two configurations, allowing a single mission to enjoy the advantages of each type of sampling. Other scenarios are also possible, subject to the laws of orbital mechanics and the constraints imposed by launch

vehicle availability and mission resources.

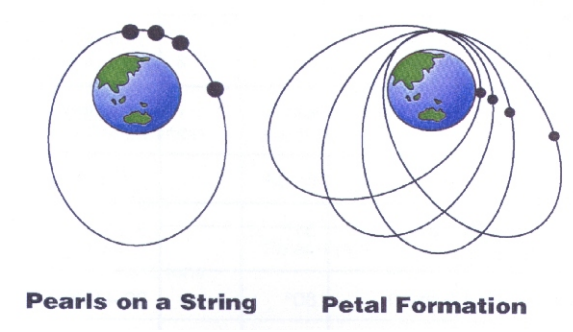

Figure 1 - Two of the possible orbital configurations for small satellite constellations. The pearls on a string mode allows sequential sampling in time of a structure at a given spatial location. The petal configuration allows a feature at a given location to be sampled over a range of altitudes. [Reproduced from reference 4]

In general, the presence of multiple satellites leads to multi-point measurements at different times and/or locations. This is the key to resolving the spatial-temporal ambiguity, which in turn enables a significant step forward in our understanding of the large-scale system dynamics.

The GEC mission plan calls for 3-4 separate satellites to resolve the spatial and temporal scales of the magnetospheric energy inputs to the thermospheric system, and the thermospheric and ionospheric responses to those inputs. To characterize all of the variables requires a sophisticated suite of instruments on each satellite. The GEC mission planning study categorizes the required measurements as shown in Table 1[4].

The parameters shown in Table 1 are engineering estimates based on previously flown instrumentation, albeit updated to allow for improvements due to modern electronic technology. As is obvious from the table, the power and mass requirements are significant. A spacecraft capable of supporting such an instrument suite would necessarily include large solar cells, active thermal control, and significant payload size to allow for instrument accommodation.

Figure 2 shows a typical instrument designed for a mission similar to GEC. The configuration illustrates current state of the art in scientific satellite instrumentation.

Table 1

Measured Parameters	Mass Estimate (kg)	Power Estimate (W)	Nominal Data Rate (kbps)
Ion temperature, density, and velocity	3.5	3.5	2.5
Neutral composition, temperature and velocity, plus ion composition	9	24	1.5
Electron temperature	1.5	2	1
Energetic ion and electron energy distributions	4	9	64
Magnetic field	2.5	3	1
Electric field	31	14	50

The figure shows a vector neutral wind instrument similar to what will be required on the GEC mission. The instrument makes measurements by admitting neutral particles from the external environment into one of several apertures, and then ionizing a fraction of these neutral atoms to allow further analysis. The resultant currents as a function of arrival angle and energy are directly related to the motion of the bulk neutral gas.

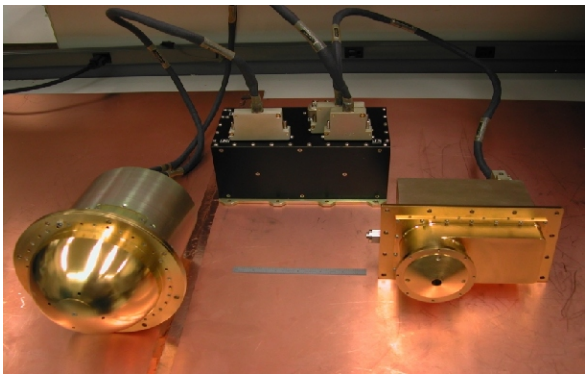

Figure 2 - The configuration of a state of the art vector neutral wind instrument, with specifications comparable to those given in Table 1. The gold box in the right foreground has physical dimensions of about 15 x 10 x 12 cm.

The device is comprised of two sensors, each with embedded electronic boards, plus a separate electronics box that provides the interface to the telemetry system and performs power conditioning functions. Although it is not obvious from Figure 2, the black box in the background contains circuit boards populated with discrete components. Such a circuit board is shown in Figure 3. The figure shows a populated board with dimensions of about 14. x 9.5 x 1 cm. This scale and fabrication method affords certain advantages in terms of radiation hardness, but severely impacts spacecraft resources due to size and power requirements.

At the right hand side of the board in Figure 3 is the electrometer, which is the heart of

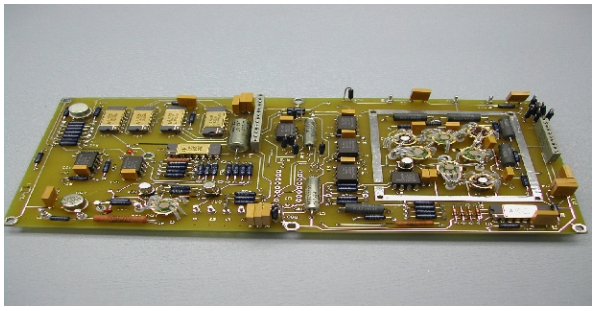

Figure 3 - A single circuit board of the type used to measure the small currents detected by the instrument shown in Figure 2. The electrometer is on the right side of the board, surrounded by a ground plane.

the instrument and the subsystem that is most sensitive to noise. The two most significant noise sources are:

1. Electronic cross-talk from other subsystems;
2. Leakage currents from through the circuit board itself.

Surrounding the electrometer assembly with a ground shield helps mitigate the first problem. The second issue is effectively dealt with by mounting the electrometer amplifiers such that their input leads do not make direct contact with the board. Figure 4 shows a close-up view of the electrometer amplifiers to illustrate this point.

Close examination of Figure 4 shows that the electrometer operational amplifiers are mounted on the circuit board upside down, and the input leads are connected to the sensor at posts that are isolated from the board by teflon stand-offs. Teflon sleeving is also used to insulate the amplifier leads from each other, as a safety precaution against accidental shorting.

Using design and fabrication processes such as these it is possible to measure currents as small as 10 pA at frequencies of a few hundred cycles/second, which provides adequate sensitivity and spatial resolution for most LEO

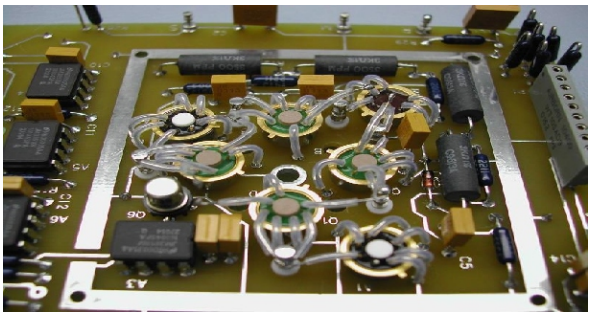

Figure 4 - Photograph of the electrometer assembly from the right side of the circuit board shown in Figure 3. The inputs are connected to the sensors using teflon stand-offs to eliminate leakage currents through the board.

scientific spaceflight missions. In the remainder of this paper we discuss the specific methodology of various measurement techniques, and we describe ongoing redesign efforts for an ion drift instrument in detail, including a comparison between on-chip instrumentation and the PC board-mounted discrete component technology illustrated in Figures 3 and 4.

Instrumentation Issues on Small Satellites

The satellites that will be at the forefront of scientific discovery over the next several decades must be substantially scaled down in order to enable deployment in constellations. Consequently, the space science instrumentation that flies on such vehicles must be less massive, use substantially less power, be physically smaller, and demand fewer payload resources.

Although it is impossible to precisely define future requirements, given that the mission scenarios are not yet known, it is prudent to begin making estimates for the purposes of planning, redesign, and development. If we assume that future missions will involve satellites of some nominal size, then we can proceed to examine the milestones that must be achieved in order to enable such missions to make useful and comprehensive scientific measurements. We will therefore make the assumption that future small satellites will fit within an envelope having a physical volume less than or equal to approximately 1.5 m^3. To perform useful scientific functions, such a platform must be capable of hosting a suite of six or more instruments (see Table 1).

Many of these instruments will have specific pointing requirements in order to achieve their scientific goals. For instance, instrumentation designed to measure vector drifts of the ionized and neutral constituents of the medium typically require mounting on the ram surface of the satellite. Subject to our working assumptions, the available surface area for mounting such instruments may be only about a meter in diameter.

Size Limitations

The sizes of the actual sensors needed for most space science instrumentation of the types we are considering is frequently determined by the requirement that charged particle collecting areas be physically large enough to collect currents in measurable ranges. For practical purposes this requires that the minimum net current flux to each sensor is on the order of 10 pA (for plasma measurements).

The total ion or electron current to a surface is given by I=NeVA, where I is the current, N is the charged particle density, e is the electronic charge, V is the normal component of the relative velocity between the satellite and the particle, and A is the area of the sensor. For a typical plasma science mission the range of meaningful particle densities ranges from about 10^7 m^{-3} to a few times 10^{12} m^{-3}, and the relative velocity (for slow-moving ions and neutrals) is comparable to the satellite velocity of 8000 m/s. Thus the instrumentation must have a dynamic range covering about five orders of magnitude, with a sensitivity to fluctuations of about 10 pA. The result is that the area of the collecting surfaces must be on the order of a few square

centimeters. Fortunately, even when guard electrodes and mechanical mounting hardware are accounted for, this constraint on overall collector size does not appear to present a significant problem subject to our assumptions about overall payload dimensions.

Power Limitations

More severe limitations become apparent when considering the power budget available for instrumentation on small satellites. As can be seen from Table 1, the power budget for the instrument complement envisioned for the GEC mission is more than 55 W. This is in addition to the power required for other necessary spacecraft subsystems, including telemetry, attitude control, onboard propulsion, thermal control, and the overall data processing unit (DPU) which interfaces to all scientific instruments.

The power available depends on the size and efficiency of the solar cells, and on the batteries carried by the spacecraft. The total spacecraft volume on future small satellite missions such as we are considering will be about one-fifth the size of the GEC satellite. If we make the simplistic, but perhaps conservative assumption that this scaling factor carries over directly to the solar cell area and battery volume, it implies that the total scientific instrument complement should consume about 10 W of spacecraft power. If it is further assumed that 5-6 instruments will be required for a synergistic, comprehensive experiment, then the milestone for instrument development should be new designs that consume less than 2 W of power. This introduces a tremendous challenge to the scientific community, but one that may be attainable by moving to on-chip designs and innovative packaging approaches.

Radiation Susceptibility

An important issue that arises when considering on-chip instrument designs to replace discrete components on printed circuit boards is the problem of radiation susceptibility. Depending on the thickness of available shielding materials and the orbital parameters of the mission, the total accumulated radiation dose received over a several year mission lifetime may range from a few kilorads to tens of megarads. Our concern here is with LEO missions, where the Earth's magnetic field introduces considerable shielding effects and limits total dosage to the lower end of this range[5]. However, even in LEO the total radiation environment varies considerably as a function of solar cycle, orbit altitude, eccentricity, and inclination.

Single event upsets from galactic cosmic rays, solar proton events, and other radiation sources can also vary widely over mission lifetime[5]. Susceptibility to single event upsets (SEUs) and single event latch-ups (SELs) are perhaps the most significant problems, and the most difficult to address. The charge carriers liberated in silicon-based semiconductors by SEU and SEL events can create spurious signals, logic gate errors, CPU halts, and even permanent instrument failure. Susceptibility to all problems of this nature grows in proportion to the density of silicon devices in the design, which is why the use of discrete components on printed circuit boards help to mitigate these issues.

As design density increases to reduce instrument size and power requirements it will be very important to find methods for dealing with these increases in radiation susceptibility. There are two obvious approaches to this problem: increasing shielding, and adding redundancy and error detection/correction circuitry. While we have not yet attempted to study this problem in detail or to perform laboratory radiation tolerance testing, it seems likely that the first approach will offer the most benefit for the least cost.

One factor that favors this approach is that the smaller on-chip designs which are inevitable in future instrumentation will allow greatly

increased shielding thicknesses with little added mass. In other words, it may be effective to combat increased radiation hazards posed to on-chip designs simply by enclosing them in thicker aluminum boxes. The dramatically smaller size of the electronics should allow this to be accomplished without large increases in payload mass. As our redesign efforts progress to the stage of fabricating test components we will investigate these approaches quantitatively and formulate specific strategies and mitigation techniques.

Specific Instruments and Redesign Issues

In order to quantitatively describe the key design concepts and illustrate realizable design improvements, we will concentrate our discussion on a particular instrument, the ion drift meter. This instrument is not the most striking case in terms of design comparisons, since it already comes very close to meeting the target design specifications (<2 W, few kg) mentioned earlier. However, it is representative of instrumentation that measures small currents in the LEO space environment, and therefore provides a valid point for comparative estimates. By extrapolation it will provide a useful reference point for scaling the specifications of other instrument designs.

First we will describe the IDM's measurement methodology and current design specifications. Then we will provide specifications for the discrete component version of the instrument. This will establish the background for comparison with the redesigned on-chip version of the instrument.

Ion Drift Meter

Figure 5 shows a schematic of the ion drift meter (IDM), which measures the bulk flow of ions perpendicular to the ram direction of the satellite. The instrument is comprised of a square aperture covered by a number of wire mesh grids. The grid system allows ions to enter the device and be collected on four identical gold-plated square collector plates, while ensuring that electrons are repelled and secondary electrons do not contribute to the net current. The four collectors are geometrically symmetric, and together comprise a square collecting area behind the grid system.

The instrument aperture faces in the ram direction, and the supersonic velocity of the spacecraft relative to the ions effectively forms a beam whose footprint falls only on a portion of the square collector surface. Since the total collector surface is segmented into four equal pieces, the ratio of the current to these segments is geometrically related to the arrival angle of the ion beam, which in turn is simply related to the ion drift perpendicular to the ram direction.

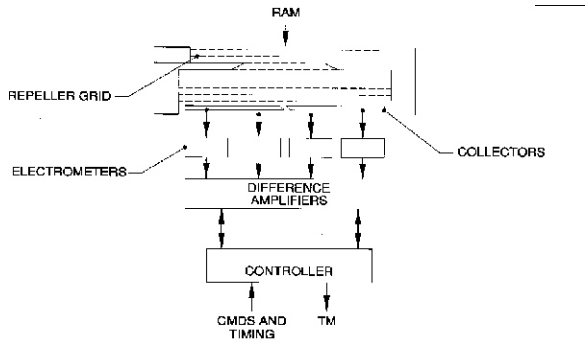

Figure 5 - Schematic diagram of the ion drift meter (IDM) instrument, which uses a segmented collector to measure the arrival angle of intercepted ions.

Aside from incremental improvements in discrete component technology, the IDM is essentially the same instrument that was originally flown on the Dynamics Explorer (DE) satellite over twenty years ago[6]. Since then it has flown successfully on many other space science missions, including the DMSP series and ROCSAT. The next flight of this version of the IDM instrument will be on the Communication/Navigation Outage Forecast System (C/NOFS) satellite, which is scheduled for launch in early 2004.

The dynamic range of the instrument that will fly as part of C/NOFS is ±500 m/s, with an accuracy of 2 m/s. Note that this stated accuracy is representative of the instrument itself, and does not include the error associated with spacecraft pointing. The IDM is sampled at 100 Hz in flight, giving an ultimate spatial resolution of about 80 meters. The instrument plus electronics measures about 12 x 12 x 9 cm, has a mass of about 2 kg, and draws about 2 W of power.

Redesign of the IDM

To conserve power and space we have begun to investigate the idea of redesigning the IDM instrument as a single integrated circuit (IC) chip. The IC design of the instrument must have the same functionality described above; namely, it measures the current ratios from the ram-facing collectors and sends the converted digital signal to the DPU (Data Processing Unit) through an SPI interface. However, due to integration, all the components are built on one chip. The resultant electronics package occupies much less space and consumes less power. The overall design block diagram is demonstrated in Figure 6.

All the power for this chip is provided by the power management unit, which consists of a bandgap reference and voltage regulator to regulate the power supplied by the satellite. It also provides a current reference for circuit biasing that is independent of temperature and supply voltage. Currents come from the four collectors, which are labelled A, B, C, and D in Figure 6. The multiplexer samples currents in pairs for each measurement, since it is the current ratio that is related to the ion arrival angle. For example, depending on the specific geometry of the collector, the horizontal arrival angle might be related via the tangent function to the ratio $(I_A+I_B)/(I_C+I_D)$, where I_A is the current to segment A, *etc*.

The current sensor calculates the ratio of the sampled currents, and this ratio is digitized by a 12-bit analog-to-digital converter (ADC). Using 12-bit resolution guarantees that the result has sufficient accuracy to meet the scientific objectives. Aside from the analog part of the design, the digital design is relatively standard. Following the ADC, the signals are synchronously clocked through a shift register to the SPI interface.

The most challenging part of the IC design of the IDM is the analog current sensor, which needs to measure input currents over a range of about five decades (100 dB). Design details of the current sensor are described in next section.

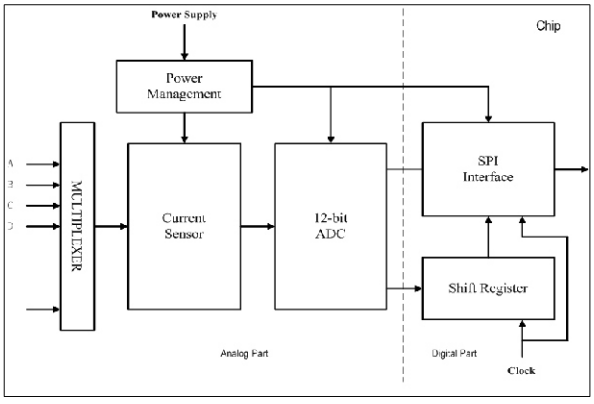

Figure 6 - Integrated IDM block diagram.

Current Sensor Design

Two distinctly different methods are under consideration for the current sensing electronics: the first uses bipolar logarithmic amplifiers, as in the original discrete component design; the other is a current integration method that has been widely used in the high dynamic range, small current measurements from photo sensors.

Log Scale Current Sensor

The log-scale current sensor generates a signal related to the ratio of its two inputs (A and B) using two logarithmic amplifiers followed by a

difference amplifier, as shown in Figure 7. The output is ln (A/B) = ln A - ln B. A traditional way to implement logarithmic technology is to use the inherent logarithmic relationship between the collector current (I_C) and the base-emitter

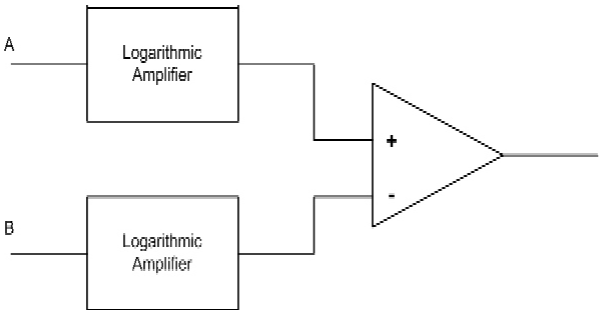

Figure 7 - Using logarithmic amplifiers to obtain the ratio of two input signals.

voltage (V_{BE}) in a bipolar transistor[7], such as Q1 in Figure 8. The functional relationship is described by

$$V_{BE} = V_T \ln(I_C / I_S) \quad (1)$$

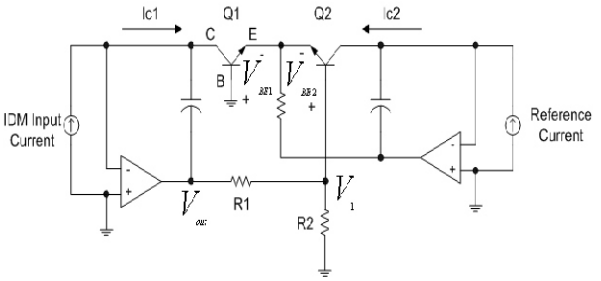

Figure 8 - Circuit diagram of a log-scale amplifier.

where V_T is the thermal voltage and I_S is a constant used to describe the transfer characteristic of the bipolar transistor in the forward-biased active region. I_S is related to device specific parameters, which can vary by 30% in IC technology from different process runs. To make the output independent of these device parameters, a reference current I_{C2} can be added as shown in Figure 8[8]. If Q1 and Q2 are matched, about 2% variation can be achieved within one fabrication run. The voltage, V_1 , which is the difference between the two bipolar base-emitter voltages, can be expressed as:

$$V_1 = V_{BE2} - V_{BE1} = -V_T \ln(I_{C1} / I_{C2}) \quad (2)$$

The output voltage (V_{out}) can then be expressed as

$$V_{OUT} = -V_T \frac{R_1 + R_2}{R_2} \ln(I_{C1} / I_{C2}) \quad (3)$$

Thus V_{OUT} is logarithmically relationed to the current ratio and is independent of device fabrication-dependent parameters.

Operational amplifier

The operational amplifier used here has rail to rail input and output capabilities[9]. Figure 9 shows the schematic, where the input stage is a fully differential folded cascade stage. The rail-to-rail input is implemented by placing an N-channel and a P-channel input pair in parallel (M1-M4), utilizing the characteristic that the N-channel and P-channel can reach the positive and negative supply rails, respectively. The three working phases of the input stage are:

1. Low common-mode input voltages; only the P-channel input pair operates.
2. Intermediate common-mode input voltages; N-channel and P-channel pairs both operate.
3. High common-mode input voltages; only the N-channel input pair operates.

The output stage is a feedforward class-AB amplifier. Transistors M13 and M14 set up a small voltage between the gates of M19 and M20, and are biased by M15-M18. Two translinear loops are therefore formed. One is composed of M13, M15, M16, M19, and the other one by

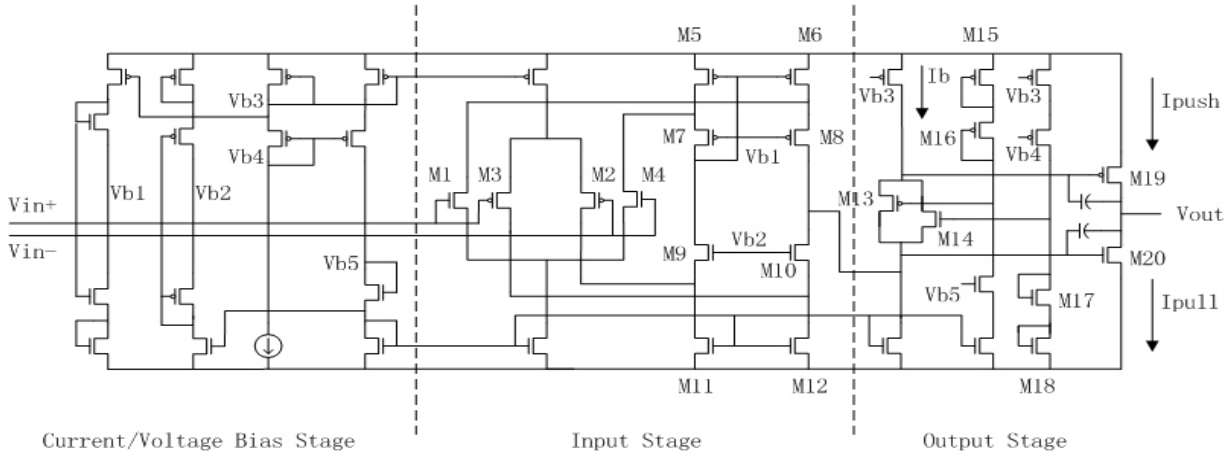

Figure 9 - Schematic of the operational amplifier used in the logarithmic electrometer design.

M14, M17, M18, M20. Thus, the voltage loop equations are:

$$V_{GS19} + V_{GS13} = V_{GS15} + V_{GS16} \quad (4)$$

and

$$V_{GS20} + V_{GS14} = V_{GS17} + V_{GS18} \quad (5)$$

When the transistor parameters are set properly a good relationship between I_{PUSH}, I_{PULL}, and the bias currents, I_b can be achieved.

An optimized result is one where the maximum value of either I_{PUSH} or I_{PULL} is around four times of the quiescent current (I_q), while the minimum is as low as 0.34 of I_q, which is defined by:

$$I_q = \frac{(W/L)_{19}}{(W/L)_{15}} I_b \quad (6)$$

where W is the channel width and L is the channel length of a MOS transistor. Thus, the amplifier has high power efficiency and can drive big loads. It is worth pointing out that the output stage is also extended to rail-to-rail range by M19 and M20.

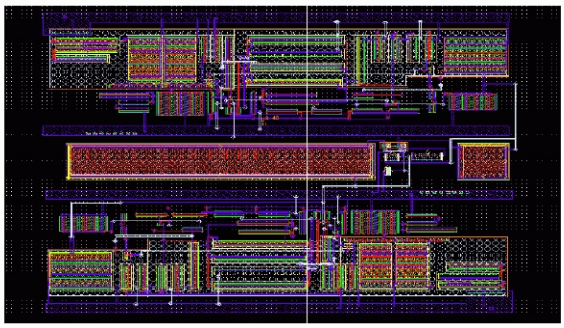

Figure 10 - Chip layout for the log-scale device.

Layout and simulation result

The layout of log-scale current measurement is shown in Figure 10, and the post-design simulation result is shown in Figure 11. The simulation result shows that the device is very linear and the dynamic range is large enough (6-decades, 120 dB) for the application.

This IC design implementation leads to an electronics package that is much smaller and consumes less power than the previous discrete version. The size of the log-scale electrometer is only 460 µm x 400 µm, and the estimated power consumption is 50mW.

For the digital portion of the instrument, we estimate the dimensions of a 12-bit ADC at about 1 mm x 1 mm, with power consumption

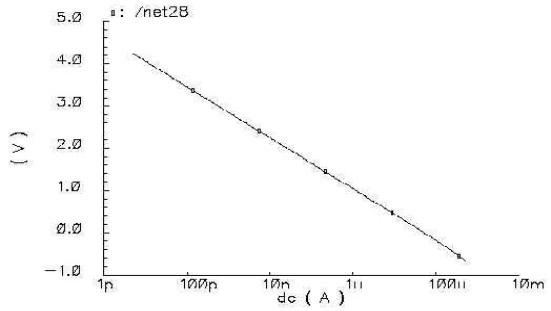

Figure 11 - Simulation result for the current-voltage characteristic of the log-amp device.

less than 10mW. When combined with the power management unit, the whole ion drift sensor could have dimensions of about 1.5 x 1.5 mm (exclusive of packaging) and consumes about 80 mW of power. Table 2 summarizes the benefits of the IC design versus the discrete component-based IDM described earlier.

Table 2

Parameter	**Discrete Component Design**	**Integrated Circuit Design**
Total Power	2 W	80 mW
Size	12 x 12 x 6 cm	3 x 3 x 1 cm with packaging

Alternative Electrometer Design

Instead of using log scale amplifiers to measure the small currents encountered in spaceflight, we are also investigating an alternative approach to using integration-based digitization, as shown in Figure 12. In this case the current to the sensor is used to charge a capacitor for a variable period of time. The governing relationship is CV=IT, where C is the capacitance, V is the voltage across the capacitor, T is the integration period, and I is the input current. For a known integration time T, the voltage V is proportional to the input current I. An ADC can be used for subsequent digitization.

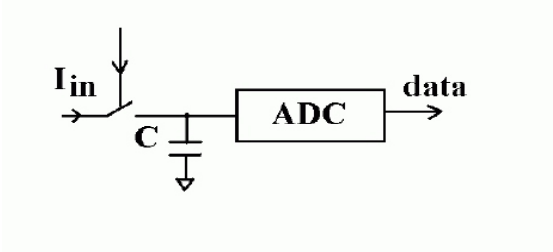

Figure 12 - Simple block diagram of the integrating scheme used for small current detection.

Compared with the log-scale voltage conversion discussed in the previous section, this approach provides a linear input-output characteristic and generally has a better signal-to-noise ratio. However, due to the circuit noise and the small voltage swing of the integrated circuit, the dynamic range is limited for a fixed integration time.

When the input current is small the voltage on the capacitor is also small, and may not be distinguishable from the noise. This is shown as the cutoff region in Figure 13. On the other hand, when the input current is too large, the voltage across the capacitor will be saturated (also illustrated in Figure 13). Normally it is difficult to achieve a dynamic range larger than 60 dB using simple integrated circuits. Since the

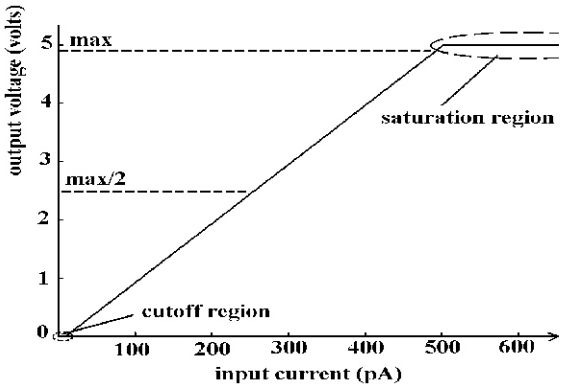

Figure 13 - Demonstration of cutoff and saturation in the integration process.

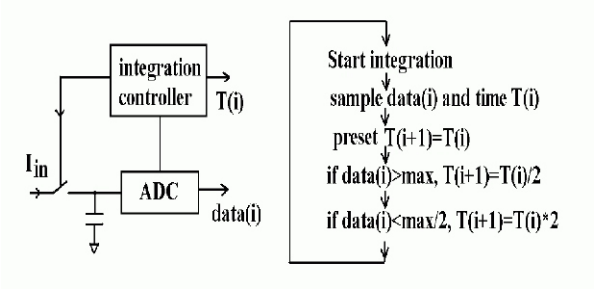

Figure 14 - Adaptive integration time algorithm.

electrometer in this application requires a dynamic range larger than 100 dB, it is necessary to use a revised design that adaptively adjusts the integration time[10, 11].

As shown in Figure 14, an integration time controller can be used to adaptively adjust the integration time based on the magnitude of the detected current. This is implemented by comparing each sampled data value to a reference, and either doubling or halving the integration time based on the outcome of the comparison.

Each time a data sample is obtained, it is compared with the value "max", which means a point near saturation. If the data sample is larger, it is assumed that the next several inputs will also be large, and the integration time T is doubled to prevent the data from being saturated. The sampled data value is also compared with max/2 - if it is smaller, the integration time is reduced to T/2. This method not only prevents the voltage from being cutoff, but also maintains the readout signal in a high voltage range so that the signal-to noise ratio remains high. The upper limit of the integration period T is simply the reciprocal of the sampling rate required by the application, which is typically less than 1 kHz for space science applications. The lower limit of the T is the speed of the integration switch, which is generally much faster than required by the application.

The adaptive scheme described here is early in the development phase, but shows much promise for application in space science measurements of small currents. It has been used previously for image sensor applications, which also present a need for small current measurements[11]. We plan to continue our exploration of this approach, and to fabricate chips incorporating both approaches for future laboratory testing.

Other Drift Instruments

The comparisons made for the IDM instrument provide a basis for extrapolation to other space science instrumentation, particularly those that utilize small current measurements to reveal details of ion and neutral drift velocities. In addition to the on-chip circuit ideas described above, systems that measure neutral particle drifts offer other avenues for power savings. This section briefly discusses several other instrument concepts, describes the present state of the art, and discusses potential miniaturization efforts that may make them more suitable for future space missions.

Retarding Potential Analyzer

The IDM instrument described above measures the two components of the ion drift that are perpendicular to the spacecraft motion. Measurements of the drift component parallel or antiparallel to the spacecraft velocity vector are

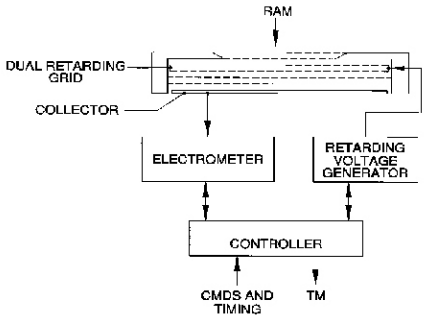

Figure 15 - Schematic diagram of a retarding potential analyzer instrument that incorporates and electrometer for measuring collected currents as a function of retarding voltage.

made using a retarding potential analyzer (RPA) technique[12].

The basic instrument concept is illustrated in Figure 15. The sensor consists of a planar current collecting surface behind a series of mesh grids. The grid system serves to exclude electrons from entering the aperture, suppress secondary emission from the collector, and perform energy analysis by sweeping one of the grid voltages through a range that encompasses the thermal ion distribution. By measuring the ion current as a function of retarding voltage on the swept grid, the mean ion energy and temperature can be determined[12].

In addition to the IDM, the C/NOFS satellite will also fly an RPA instrument. Like the IDM, it is already fairly light and consumes a small amount of power. It has the same physical dimensions and mass as the IDM and consumes roughly the same amount of power. The resolution and accuracy are also comparable to the IDM instrument. Extrapolations based on IC design results for the RPA instrument are therefore very similar to those shown in Table 2 for the IDM.

Neutral Drift Instruments

Instruments designed to measure neutral drifts both parallel and perpendicular to the satellite trajectory introduce some new issues to the miniaturization process. However, it is possible to use the same basic approach used in the IDM and RPA schemes to measure neutral particle flow velocities from a satellite platform. This is being attempted for the first time on the C/NOFS mission, but the technique is expected to be included in the GEC mission as well. The main differences are:

1. For the ram-directed drift measurement a fraction of the neutral particles entering the instrument must be ionized prior to performing the retarding potential analysis.
2. For the cross-track drifts the differential pressure between adjacent chambers is measured (rather than a ratio of currents falling on a segmented collector).

The range of current magnitudes that must be measured in both cases is roughly the same, so the electrometer designs for both neutral and ion instruments can be very similar. As a consequence of this, the techniques discussed above for the on-chip electrometer can be applied to neutral measurements as well. Figures 16 and 17 show the schematic design of the ram and cross track neutral wind instruments, respectively.

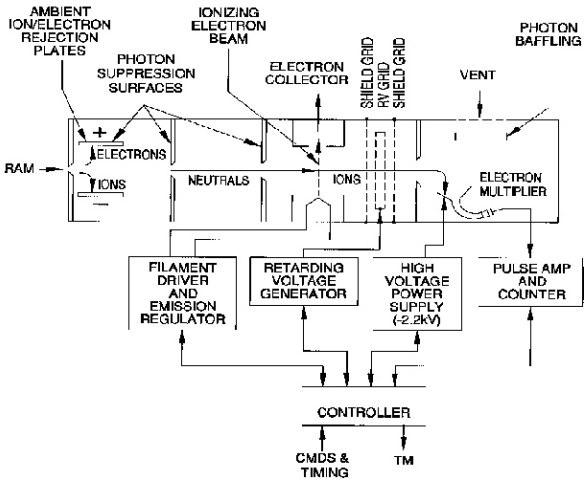

Figure 16 - Functional block diagram of the ram wind instrument to be flown on the C/NOFS satellite in early 2004 (see Figure 2 for a photograph).

The present state of the art for the vector neutral wind instrument, which combines the ram and cross-track sensors, is an instrument that has a mass of 5.6 kg, measures 22 x 12 x 10 cm, and draws 10 W of power. The flight version of this instrument was pictured in Figure 2 as a representation of all instruments of this class. Its dynamic range is ±500 m/s, and it is accurate to within ±5 m/s. The main reason for the large power consumed by this instrument relative to the ion instruments is the presence of Tungsten-based filaments. In the ram velocity sensor a filament is used to ionize a portion of the incoming neutral

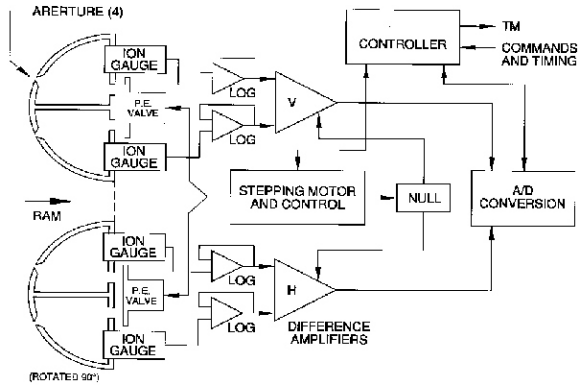

Figure 17 - Functional block diagram of the cross track neutral wind sensor (also see Figure 2).

stream, while in the cross-track velocity sensor four separate filaments are used in the Bayard-Alpert type pressure sensors that measure the pressure in each chamber.

In addition to moving toward on-chip electrometers and associated electronics, we envision future neutral particle flow instruments that utilize microtip or nanotube emitters in place of filaments[13]. Figure 18 shows an electron micrograph image of a nanotube emitter. The drawbacks to using such emitters are presently the requirements for cleanliness and bake-out prior to use, and their questionable robustness in corrosive oxygen environments. The bake-out and cleanliness issues are difficult to accommodate in a spacecraft environment without the use of considerable extra satellite resources, but it may be feasible to address these concerns using vacuum-sealed instruments with deployable covers. The corrosive nature of the medium will prove more difficult to address, although newer materials may help mitigate this concern. Research is ongoing at many institutions to test this hypothesis.

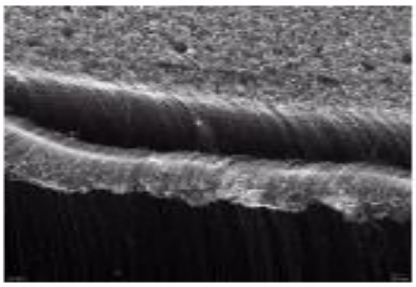

Figure 18 - An SEM image of carbon nanotubes fabricated in a carefully aligned array.

Extrapolated Design Estimates

The filament systems that measure pressures in the neutral drift instruments consume roughly 7 W of power. To produce the same electron flux using a microtip or nanotube emitter requires approximately 50 mW. Assuming that the technical problems surrounding the use of nanotubes or other cold emission devices in space can be solved, it should be feasible to redesign the vector wind instruments such that they draw less than 2 W, and occupy about half the volume of the instrument shown in Figure 2.

Summary and Conclusions

The results presented here are admittedly preliminary, since we have only recently begun to investigate the potential benefits of on-chip designs and have not yet built a device for laboratory testing. However, the results so far are encouraging in that they indicate the feasibility of using IC devices to measure small (pA order) currents at rates of about 100 Hz - 1 kHz.

Our initial estimates show that it should be possible to cover the wide dynamic range required for space science measurements, without sacrificing accuracy, linearity, or spatial resolution. In the coming months we plan to fabricate a number of such chips, and to perform detailed tests for direct comparison to the discrete component design now in use. Additional tests will include radiation exposure tests and shielding

studies to parameterize the effects of high energy particles on IC chip performance.

Smaller, lighter, and less powerful satellite payloads are already being developed, and plans to launch constellations of such payloads will soon be approved and funded. As this new era begins in space science, we plan to meet the instrumentation challenges by fielding a new generation of smaller, more efficient space science instruments. The new experiment scenarios that can be envisioned for these small satellite constellations are certain lead to new discoveries and improved understanding of the near-Earth space environment.

Acknowledgments. This work was supported by NASA grant NAG5-10335.

References

1. Fejer, B. G., "The Electrodynamics of the Low-Latitude Ionosphere: Recent Results and Future Challenges", Journal of Atmospheric and Solar-Terrestrial Physics, vol. 59., no. 13, p. 1465, 1997.
2. Wescott, E. M., *et al.*, "Triangulation of Sprites, Associated Halos and Their Possible Relation to Causative Lightning and Micrometeors", Journal of Geophysical Research, vol. 106, no. A6, p. 10,467, 2001.
3. Conde, M., *et al.*, "Assimilated Observations of Thermospheric Winds, the Aurora, and Ionospheric Currents over Alaska", Journal of Geophysical Research, vol. 106, no. A6, p. 10,493, 2001.
4. Report of the NASA Science and Technology Definition Team for the Geospace Electrodynamic Connections (GEC) Mission, NASA/TM-2001-209980, July 2001.
5. Tascione, Thomas F., Introduction to the Space Environment, Orbit Press, Malabar, FL, 1988.
6. Heelis, R. A., *et al.*, "The Ion Drift Meter for Dynamics Explorer-B", Space Science Instrumentation, vol. 5, no. 4, p. 511, 1981.
7. Gray, Paul R., *et al.*, Analysis and Design of Analog Integrated Circuits, Wiley, 4th edition, New York, 2001.
8. Kennedy, E. J., "Low Current Measurements Using Transistor Logarithmic DC Electrometers", IEEE Transactions on Nuclear Science, v. NS-17, p. 326, 1970.
9. Hogervorst, R., *et al.,* "A Compact Power-Efficient 3 V CMOS Rail-to-Rail Input/Output Operational Amplifier for VLSI Cell Libraries", IEEE Journal of Solid-State Circuits, v. 29, number 12, p. 1505, 1994.
10. Yang, D., and A. El Gamal, "Comparative Analysis of SNR for Image Sensors with Enhanced Dynamic Range", Proceedings of the SPIE on Electronic Imaging, v. 3649, p. 197, San Jose, CA, 1999.
11. Chen, Sarit, and R. Ginosar, "Adaptive Sensitivity CCD Image Sensor", Proceedings of the 12th IAPR International Conference on Signal Processing, v. 3, p. 363, 1994.
12. Hanson, W. B., *et al.*, "The Retarding-Potential Analyzer on Atmosphere Explorer", Radio Science, vol. 8, no. 4, p. 333, 1973.
13. Brodie, Ivor, and Paul Schwoebel, "Vacuum Microelectronic Devices", Proceedings of the IEEE, vol. 82, no. 7, 1994.